Electronic structure and Fermi surface of UNZ (Z=Se and Te) by *ab initio* calculations

M. Samsel-Czekała
Institute of Low Temperature and Structure Research, Polish Academy of Sciences, P.O. Box 1410, 50-950 Wrocław 2, Poland and Leibniz-Institut für Festkörper- und Werkstoffforschung, IFW Dresden, PF 270116, D-01171 Dresden, Germany
(Received 23 December 2009; revised manuscript received 29 April 2010; published 20 May 2010)

The electronic structures of ferromagnetic (FM) UNTe and its nonmagnetically ordered (NMO) isostructural (tetragonal $P4/nmm$) and isoelectronic counterpart, UNSe, have been calculated from first principles in the framework of the fully relativistic and full-potential local-orbital band-structure code within local-spin density approximation (LSDA) including also an orbital polarization correction by Eriksson, Brooks, and Johansson (OPB). The results predict that both ternaries have a covalently metallic character and solely uranium atoms, located in (001) planes, form a metallic bond due to the U $5f$-$6d$ electrons. The U $5f$ electrons contribute also to a covalent bond with the ligand N and Te or Se atoms and they reveal a *dual* character, i.e., partly localized and itinerant. Contrary to UNSe, UNTe is a collinear FM with the magnetic moment alignment along the c axis, as observed experimentally in the past and now is well reproduced by the LSDA+OPB calculations. In NMO states of both systems, band pseudogaps are opening merely ~0.25 eV below the Fermi level, which cause an instability of the metallic state under small perturbations leading to a semiconducting behavior. The two-band Fermi surfaces (FSs) of both compounds (in NMO state) have similar quasi-two-dimensional (Q2D) properties with nesting vectors along the [100] direction. In turn, UNTe in the FM state possesses three-band FS with also Q2D properties and nesting features along the [100] and [110] directions, being important, e.g., in arising such collective phenomena as superconductivity.

DOI: 10.1103/PhysRevB.81.195115 PACS number(s): 71.27.+a, 71.20.−b, 71.18.+y, 75.50.Cc

I. INTRODUCTION

The UNZ-type (Z=Se,Te) compounds adopt the tetragonal crystal structure of the PbFCl-type (space group: $P4/nmm$, no. 129) (Refs. 1 and 2) (see Fig. 2 in the next section) and, in addition, are isoelectronic possessing the same kinds and number of valence electrons but originating from different electron shells: $4s^24p^4$ and $5s^25p^4$, for Z=Se and Te, respectively. The primary magnetic measurements, curried out a long time ago by Troć and Żołnierek,[2,3] showed that the magnetic susceptibility of UNSe in the paramagnetic region increases rapidly below T=140 K due to arising a short magnetic order, while UNTe behaves as a strongly anisotropic ferromagnet with the Curie temperature T_C =54±2 K. A comparison of the magnetization results for both compounds (taken from Ref. 3), obtained at 4.2 K and in magnetic fields up to 5 T shows that the magnetization of UNSe, despite a much enhanced magnetic susceptibility at lower temperatures, is linear in applied magnetic field strengths as for a nonmagnetically ordered (NMO) state. In contrast, the magnetization of UNTe increases with magnetic field typically for a ferromagnet achieving, in fields above 3 T, a tendency to saturation into a value of about $0.6\mu_B$. This powder value in the statistical condition would then correspond to about $1.2\mu_B$ in the case of an easy magnetization axis c of a uniaxial ferromagnet. Next, Amoretti *et al.*[4] based on neutron powder diffraction and heat capacity studies proved both an absence of a magnetic order in UNSe, at least down to 4.2 K, and an appearance of a simple collinear ferromagnetic (FM) ordering in UNTe with its magnetic moments arranged along the elongated c axis (c/a is of 1.91). The total ordered magnetic moment per an uranium atom, inferred from the neutron powder study of UNTe at 4.2 K amounts to μ_{tot}= 0.85±0.16μ_B,[4] i.e., is considerably lower than that roughly predicted from the powder magnetization measurements. This discrepancy probably arises from a nonstatistical spreading of FM grains in a compressed powder sample[3] used in the magnetization measurements. In the paramagnetic range (but for UNSe above 150 K) both considered here ternaries behave in a similar way following a modified Curie-Weiss law with an effective magnetic moment ~2.0μ_B.[3,5] In turn, the heat-capacity measurements were also in accordance with the above findings and yielded medium and fairly large electronic specific-heat coefficient, $\gamma(0)$, values, i.e., 22 and 60 mJ K^{-2} mol^{-1} for UNTe and UNSe, respectively,[4] comparable to that in UN-$\gamma(0)$ =49 mJ K^{-2} mol^{-1}.[6] The value of $\gamma(0)$ in UNSe is characteristic of magnetically correlated metals exhibiting only a NMO state while that in UNTe is much smaller due to the occurrence in this system of the FM order. Unfortunately, no transport measurements of the UN(Se,Te) ternaries have been done so far because in the past these compounds were available only as powders. However, nowadays advanced technological (flux or chemical transport) methods of preparation can be used to produce their thin films or bulk samples even in the form of single crystals.

Also such compounds, combining uranium with nitrogen [see, e.g., large number of papers on UN (Ref. 6)] or oxygen as are the oxychalcogenides of the UOY type (Y =S, Se, Te),[5] being isostructural with the investigated here nitrochalcogenides of the UNZ type, arise a great interest in the specific chemical bonding influencing their magnetism. This paper is a continuation of such a question studied in our previous works on UN (Ref. 7) and other nitroternaries U_2N_2(Sb,Te,Bi).[8] Interestingly, among all aforementioned compounds, only UNTe is a ferromagnet and UNSe is a strongly correlated paramagnet (such a ternary but containing sulfur, UNS, does not exist at all[2]) whereas UN and these three oxychalcogenides (UOY) exhibit an antiferromagnetic

 ©2010 The American Physical Society

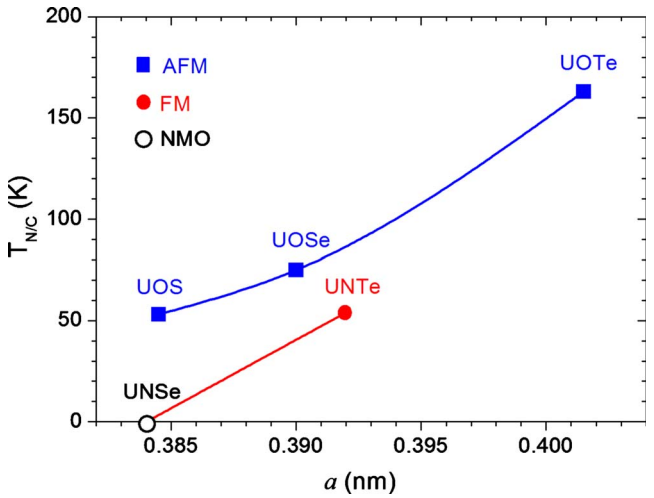

FIG. 1. (Color online) Ordering temperatures, $T_{N/C}$, as a function of the lattice parameter a for UNZ- and UOY-type ternaries crystallizing in the PbFCl-type structure (see Fig. 2), based on Fig. 8 in Ref. 3. Symbols represent FM and AFM or NMO states.

(AFM) ordering. For these materials, Fig. 1 illustrates the ordering temperatures vs the lattice parameter a, corresponding to the nearest U-U distance but in the (001) plane. Thus, the band structure calculations are a challenge for any further experiments on this type of materials. Up to now, no results of such computations for the investigated here UNZ-type or even wider probed UOY-type compounds have been published.

In the present paper, to study a kind of a chemical bond and an origin of the ferromagnetic ordering in UNTe, its electronic and magnetic structures in comparison with the reference paramagnetic compound, UNSe, have been calculated based on the density-functional theory.[9] The fully relativistic and full potential local-orbital (FPLO) code[10] was applied within the local- (spin-) density approximation [L(S)DA] with and without applying the orbital polarization (OP) correction proposed by Eriksson, Brooks, and Johansson (OPB).[11]

The experimental lattice parameters and atomic positions, previously obtained in the powder x-ray and neutron-diffraction experiments of these ternaries,[1,4] were taken to determine band energies, $E_n(\mathbf{k})$, densities of states (DOSs), Fermi surfaces (FSs), occupation numbers, and ordered magnetic moments.

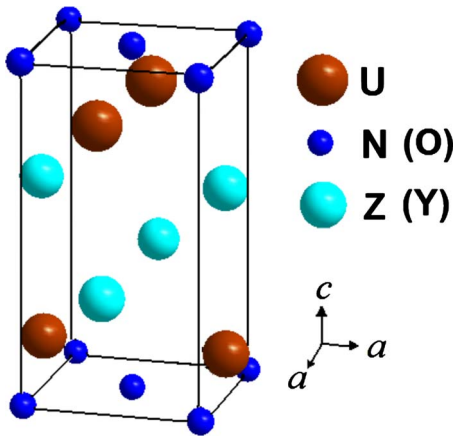

FIG. 2. (Color online) Tetragonal crystal structure of the PbFCl-type ($P4/nmm$) adopted by UNZ- or UOY-type systems, having usually $c/a<2$ and $u<0.23$ (Ref. 13) in contrast to the ZrSiS-type structure adopted by UXY-type (X=P, As, Sb, Bi) ternaries (Ref. 4).

II. COMPUTATIONAL DETAILS

The band structures of the UN(Se,Te) systems have been calculated by the fully relativistic versions of the FPLO code.[10] In this advanced method the four-component Kohn-Sham-Dirac equation, containing implicitly spin-orbit (SO) coupling up to all orders, is solved self-consistently. The Perdew-Wang parametrization[12] of the exchange-correlation potential was used in the LSDA approximation with and without the OPB correction[11] applied to the U 5f electrons. The OPB is a modified Brooks' correction (analogous to the spin polarization) in which the therm $-1/2\Sigma \boldsymbol{l}_i \cdot \boldsymbol{l}_j$ ($\boldsymbol{l}_i$ is an angular momentum for ith electron in the f^n configuration) occurring in the energy of the ground state of an atom as a function of an occupation number is replaced with $-1/2(\Sigma i l_i^z)(\Sigma j l_j^z)$ and, as a consequence, a term $\Delta E_l = -1/2E^3L^2$ is obtained where L is the total angular momentum and E^3 is a constant so-called Racah parameter.

In the computations, the x-ray experimental lattice, a and c, and free, u and v, parameters from Refs. 1 and 4, given in Table I, were used. The tetragonal crystal structure of UNZ- (or UOY)-type ternaries is visualized in Fig. 2. For UNSe, the u and v parameters were not available in the literature, hence, they were assumed the same as in UNTe (one expects very similar real values in both compounds). The unit cell of each studied system contains double formula unit (f.u.) and the following nonequivalent atomic positions are occupied:

TABLE I. Experimental lattice, a and c (in nanometer), and free, u and v, parameters in UNZ-type systems, used in calculations, and the nearest distances between U atoms, $d_{U\text{-}U}$.

System	Method	Temp.	a	c	u	v	c/a	$d_{U\text{-}U}$
UNSe	x-ray	RT	0.384[a]	0.694[a]	0.165[b]	0.624[b]	1.81	0.3552
UNTe	x-ray	RT	0.3929[b]	0.7617[b]	0.165[b]	0.624[b]	1.94	0.3747
	Neutr. diff.	20 K	0.39157[a]	0.7485[a]	0.155[a]	0.633[a]	1.91	0.3613
		100 K	0.39168[a]	0.7495[a]	0.155[a]	0.631[a]	1.91	0.3615

[a]Reference 4.
[b]Reference 1.

U [2(c)]: $(1/4,1/4,u)$; N [2(a)]: (3/4,1/4,0); and Z [2(c)]: $(1/4,1/4,v)$. The adopted valence basis sets were as follows: the U:$5f$;$6s6p6d$;$7s7p$; Se:$3d$;$4s4p$, Te:$4d$;$5s5p$, and N:$2s2p$;$3d$ states. The size of the **k**-point mesh used in the Brillouin zone (BZ) of $(12\times12\times12)$ was sufficient.

For both the NMO and FM states, total, E_{tot}, and band, $E_{\text{n}}(\mathbf{k})$, energies, occupation numbers, total and partial DOSs for each atomic site and for different electron states, as well as ordered magnetic moments have been determined within the LDA as well as spin- and orbital-polarized LSDA and LSDA+OPB approaches.

III. RESULTS AND DISCUSSION

The calculated band energies, $E_{\text{n}}(\mathbf{k})$, of the UN(Se, Te) compounds in the NMO (LDA) states are displayed in Fig. 3. Additionally, these functions for UNTe in the FM states for the magnetic moment arranged along the c axis, obtained by employing the LSDA and LSDA+OPB approaches, have been plotted in Fig. 4. All presented results for UNTe are based on the lattice parameters, determined in the neutron diffraction studies at 20 K (Ref. 4) and collected in Table I (in Sec. II), which minimize the total energy of this system within all computational approaches. It turned out that for UNSe it was not possible to achieve any stable (self-consistent) magnetically ordered state, in agreement with the experimental data described in the Introduction. One of the reasons is that the nearest interatomic uranium distance, $d_{\text{U-U}}$ of 0.355 nm (see Table I) in this compound, is just on the border of so-called Hill limit of about 0.35 nm being the critical distance for localization against delocalization of the U $5f$ electrons. Thus, the $5f$ electrons in the selenide should be stronger delocalized compared to those in UNTe with slightly longer $d_{\text{U-U}}$ distance of 0.37 nm supporting the occurrence of the FM order. The $E_{\text{n}}(\mathbf{k})$ dependencies (LDA) in UNSe are almost identical to that for UNTe in the energy scale of Fig. 3(a), hence, they are shown in Fig. 3(c) only in the vicinity of the Fermi level, E_{F}, where small differences compared to UNTe [Fig. 3(b)] are visible.

As Fig. 3 indicates (see also Fig. 8), UN(Se,Te) have two conduction bands (being Kramers double degenerated) in their NMO states. In turn, the number of conduction (nondegenerated) bands in UNTe in its FM states, based on the LSDA and LSDA+OPB approaches, amounts to three—see Fig. 4 (and also Fig. 9). Hence, both systems should be basically metallic and their conduction bands have predominantly a $5f$ electron character. However, in the NMO phases of the considered ternaries, the bottoms of the conduction bands are situated merely about 0.27 eV below E_{F}, which is also clearly seen in their DOSs presented in Fig. 6. As these figures, plotted for UNTe and UNSe, indicate, the large pseudogaps are opening just below and above their very narrow (of 0.5 eV) conduction bands. They are the most pronounced at about −0.27 and 0.25 eV, the latter being due to the SO splitting. In Figs. 3 and 4, these pseudogaps are denoted by colors numbered 3 and 1, respectively. Hence, on the one hand, such a metallic state can be unstable, being very sensitive to even small changes in values of the lattice parameters, deviation from the stoichiometry or some impurities that may drive the investigated here compounds toward a semiconducting behavior [as in UOSe or UOS (Ref. 5)]. The situation is analogous to the theoretical results obtained for the $U_2N_2(Sb,Te,Bi)$ systems in Ref. 8. On the other hand, here as also in the metallic compound UN,[7] quite large values of experimental electronic specific-heat coefficients, discussed in Sec. I, point to a metallic behavior. For UNSe, this value (60 mJ K^{-2} mol^{-1}) is typical of a strongly correlated metal, being about 2.5 times enhanced with respect to the calculated one, $\gamma_{\text{b(LDA)}}=23.6$ mJ K^{-2} mol^{-1}. Contrastingly, for UNTe the computed value of $\gamma_{\text{b(LDA)}}=35.5$ mJ K^{-2} mol^{-1} in the NMO state is higher than its experimental value (22 mJ K^{-2} mol^{-1}) and also than $\gamma_{\text{b(LDA)}}$ for UNSe. However, this coefficients calculated for UNTe in the FM states, based on the LSDA and LSDA+OPB approaches, have substantially reduced values, $\gamma_{\text{b(LSDA)}}=14.4$ mJ K^{-2} mol^{-1} and $\gamma_{\text{b(OPB)}}=7.7$ mJ K^{-2} mol^{-1}, being

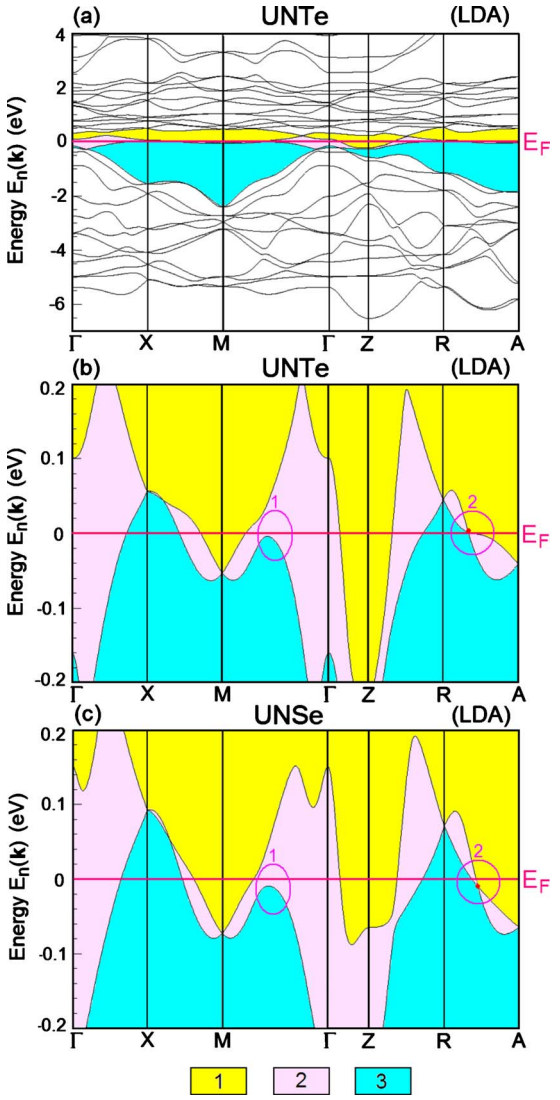

FIG. 3. (Color online) Computed band energies, $E_{\text{n}}(\mathbf{k})$, in the NMO state (LDA) for UNTe, drawn in broad (a) and narrow (b) energy regions, and UNSe (c). Pseudogaps at E_{F} and narrow area between them are shaded by colors numbered as (1,2,3) in legend. Instability points in ellipses are discussed in the text.

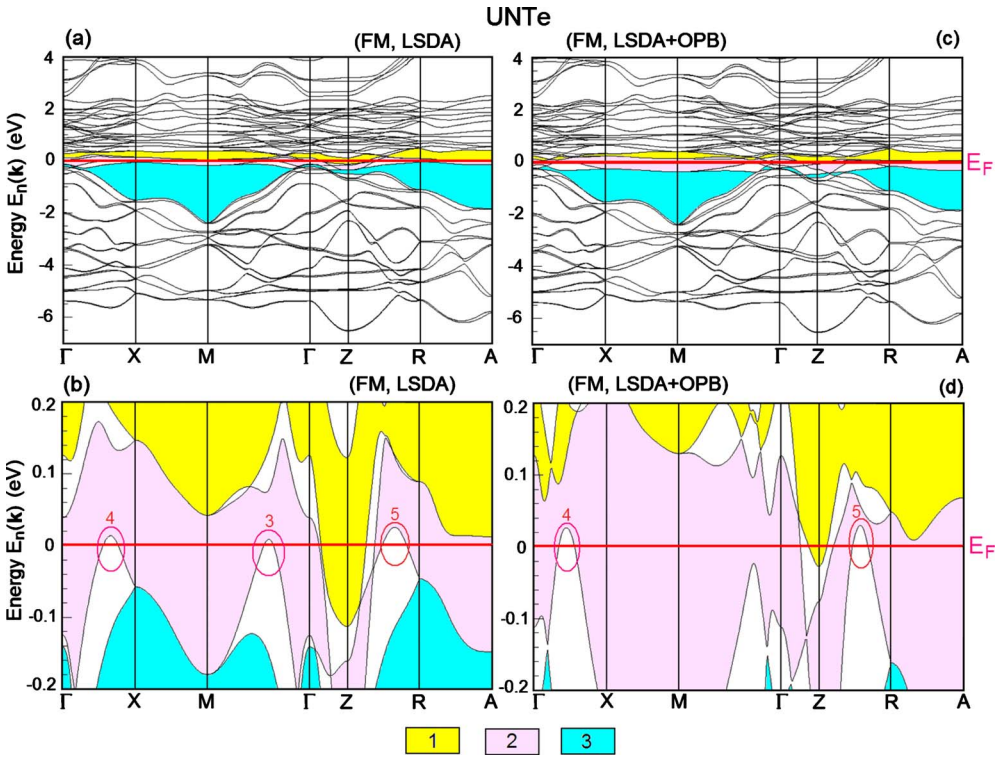

FIG. 4. (Color online) Same as in Fig. 3 but for UNTe in the FM state, calculated within: [(a) and (b)] LSDA and [(c) and (d)] LSDA+OPB approaches.

much smaller than its experimental value and the $\gamma_{b(LDA)}$ for UNSe. Hence, the general $\gamma(0)$ trend in both ternaries is well reproduced by the band-structure calculations.

The band structures, $E_n(\mathbf{k})$, in both systems in the NMO states (LDA), presented on the expanded scales in Figs. 3(b) and 3(c), are very similar. However, for UNTe there are more unstable points compared to that in UNSe, namely, an intersection point of bands along the RA line and the top of a conduction band along the ΓM line, located just at E_F, marked in Fig. 3(b) by ellipses no. 2 and 1, respectively. These features disappear in UNTe after introducing the spin and orbital polarizations (LSDA or LSDA+OPB) [see Figs. 4(b) and 4(d)], and total energy is lower than in the LDA case as given below. Nevertheless, the LSDA state [Fig. 4(b)], in which two tops of conduction bands are situated again close to E_F (along ΓM and ΓX lines), denoted by ellipses no. 3 and 4, respectively, is less stable than the LSDA+OPB state [Fig. 4(d)] with tops of bands (ellipses no. 4 and 5), located ~0.03 eV above E_F. The latter state with the total energy (−950085.2555 eV/f.u.) lower by about 65 and 78 meV/f.u. than those achieved in the LSDA (−950085.1902 eV/f.u.) and LDA (−950085.1779 eV/f.u.) states, respectively, is the ground state.

In addition, Figs. 4(a), 4(c), and 7 demonstrate that in UNTe in the LSDA+OPB approach, the pseudogap dip in DOS is shifted from −0.27 eV (LDA or LSDA) to ~−0.38 eV and the SO pseudogap at 0.25 eV is reduced, which is connected with a remarkable broadening of the conduction bandwidth leading to a stabilization of the metallic behavior at low temperatures.

The computed total and partial DOSs of UN(Te,Se) are plotted in Figs. 5–7. The NMO (LDA) results are presented in Fig. 5 for all valence bands ranging down to about 19.5 eV below E_F. In UNTe, these dispersive bands remain almost unchanged (at least below −1.0 eV) in FM states. As seen, in both compounds the deepest valence bands occurring in the range of about 19.5–16.5 eV below E_F contain the contributions of the U 6*p* electrons slightly hybridized with the N 2*s* electrons and by this forming a covalent bond between the U and N atoms. The succeeding bands, in ranges of 14.5–10.5 and 14.5–11.5 eV below E_F in UNTe and UNSe, respectively, consist of dominating contributions of the U 6*p* electrons, being hybridized with the N 2*s*, and the Te 5*s* or Se 4*s* electrons that all together create a covalent bond between all three kinds of atoms. The bottoms of the succeeding valence

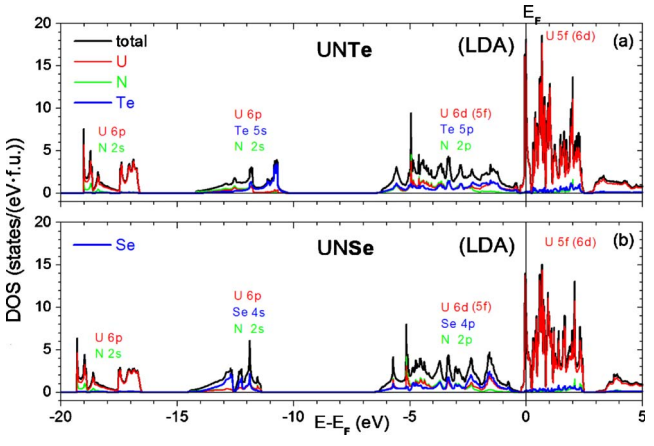

FIG. 5. (Color online) Total and partial DOSs, (per given atom and orbital), computed for NMO (LDA) states in: (a) UNTe and (b) UNSe.

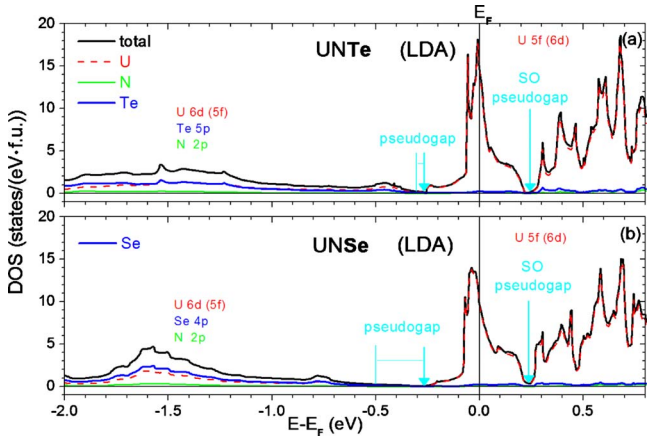

FIG. 6. (Color online) Same as in Fig. 5 but on expanded energy scale around E_F.

bands occur at 6.5 eV below E_F in both systems. As Fig. 5 illustrates, these bands originate mainly from the U 6*d* electrons being hybridized with the U 5*f* electrons and they together with the N 2*p* and Te 5*p* or Se 4*p* electrons form a covalentlike bond between all three kinds of atoms. These valence bands are separated from the conduction bands by the aforementioned pseudogaps opening at ~0.3 and 0.5 eV below E_F in UNTe and UNSe, respectively, and ranging to ~−0.25 eV. The DOSs in UNTe, in the range of 19.0–2.0 eV below E_F, resembles that in U_2N_2Te, presented in Ref. 8.

Figures 6 and 7 indicate that the conduction bands around E_F in both ternaries contain mainly the U 5*f* electrons with a negligible amount of the U 6*d* electrons. Hence, the only uranium atoms form predominantly a metallic bond. Furthermore, these states together with the U 6*p*, N 2*sp*, and *Z* (4–5)*sp* electrons contribute to a covalent bond between all kinds of atoms.

For these systems, calculations carried out for all considered NMO and FM states yielded the same mixed character

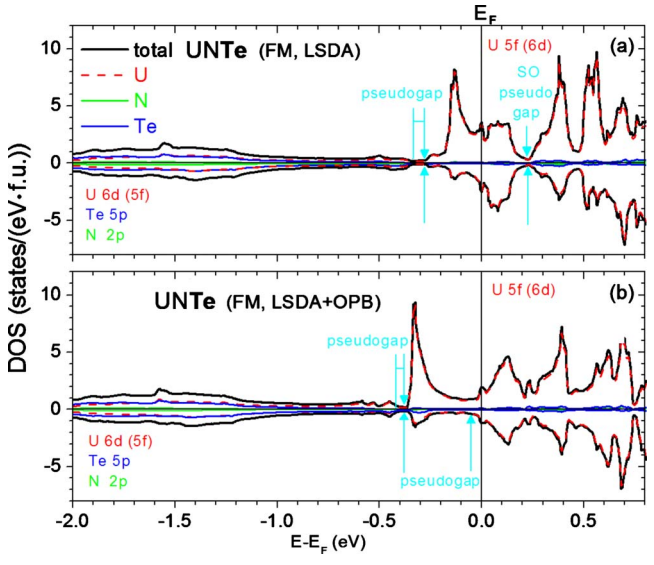

FIG. 7. (Color online) Total and partial DOSs of UNTe in FM states, computed employing: (a) LSDA and (b) LSDA+OPB approaches. Spin-up and spin-down channels are plotted separately.

of chemical bonding. This scenario is analogous to that in previously investigated systems combining uranium with nitrogen atoms, i.e., UN (Ref. 7) and U_2N_2(Sb,Te,Bi) (Ref. 8) where also solely the U atoms (due to U 5*f* and 6*d* electrons) form a metallic bond while there exist a purely covalent bond between the U and N atoms.

The overall NMO (LDA) DOSs for UN(Se,Te) are similar but only in UNTe the Fermi level cuts the top of the highest U 5*f* peak of DOSs and, hence, the NMO state becomes unstable. Moreover, the discussed pseudogap below E_F is much broader in UNSe. The DOSs of UNTe in the FM state, obtained in the LSDA approach, are displayed in Fig. 7(a). As is apparent, the majority (up) spins originating from the U 5*f* electrons are dominating in the energy region ranging from the pseudogap at ~−0.27 eV up to the Fermi level but at E_F itself the DOS peaks have relatively small and comparable intensities of 3 states/(eV f.u.) in both the spin-up and spin-down channels. In this region, the highest DOS peak, coming from the U 5*f* spin-up electrons, is centered at ~−0.13 eV. Analogous U 5*f* peaks, but being more separated by pseudogaps from other 5*f* peaks located near E_F, were observed in U_2N_2(Sb,Te,Bi) ternaries.[8] Their presence can be attributed to a formation of more localized states among the U 5*f* electrons, which give rise to their *dual* behavior, i.e., exhibiting partly localized and partly itinerant nature, as it was documented, e.g., in UPd_2Al_3 by different experiments and explained by the dual models.[14]

Finally, the DOS results obtained for UNTe in its FM state employing the LSDA+OPB approach are presented in Fig. 7(b). As shown, the bottoms of the conduction bands are shifted by about 0.1 eV, i.e., down to 0.38 eV below E_F. The highest DOS peak below E_F, present also in the LSDA results, changed distinctly its position to about 0.32 eV below E_F and even enhanced its intensity by the factor of 1.2. Again, the majority spins of the U 5*f* (and U 6*d* electrons) are dominating in the energy region from −0.38 eV up to E_F, but starting from −0.25 eV up to E_F, a broad pseudogap opens, with almost zero values of the spin-down DOSs and also small spin-up DOS of 1 state/(eV f.u.). Hence, UNTe is on the border to have a unique *half-metallic* behavior analogous to that of U_2N_2Te reported in Ref. 8.

The electron populations, N_{calc}, in the UNZ-type compounds (Z=Te,Se) in the NMO (LDA) state compared to those for the free atoms, N_{at}, are collected in Table II. N_{calc} of electrons in U and N atoms are similar in both systems (with differences ≤0.2). The U 5*f* states, having N_{calc}~3, can be regarded as rather weakly hybridized with other states and the $5f^3$ state of U atom should be stable. For the U 6*d* states $N_{calc} \cong 2 \times N_{at}$ while for the U 7*s* states $N_{calc} \ll N_{at}$. Furthermore, in N, Se, and Te atoms their s electrons have $N_{calc} < N_{at}$ while for *p* electrons $N_{calc} > N_{at}$.

This points to a charge transfer of ~0.5 valence electrons (per f.u.) from uranium to both nitrogen (of 0.23) and selenium (0.27) atoms in UNSe while in UNTe this transfer amounts to ~0.2 electrons from the U to both N (0.16) and Te (0.04) atoms. Both kinds of spin- and orbital-polarized calculations for UNTe yield identical (within accuracy of 0.1) results to those collected in Table II.

Next, the Fermi surfaces of the NMO state of the UNTe and UNSe systems, determined by the LDA treatment, are

TABLE II. Computed electron occupation numbers (per atom) in the UNZ-type compounds (Z=Te,Se), N_{calc}, in the NMO (LDA) state and that in free atoms, N_{at}, with accuracy to ± 0.1.

Electron orbitals	N_{at}	N_{calc} of UNTe	N_{calc} of UNSe
U 5*f*	3	3.1	2.9
U 6*d*	1	2.2	2.1
U 7*s*	2	0.4	0.3
U 7*p*	0	0.2	0.1
N 2*s*	2	1.6	1.6
N 2*p*	3	3.5	3.7
Se 4*s*	2		1.9
Se 4*p*	4		4.4
Te 5*s*	2	1.9	
Te 5*p*	4	4.1	

displayed in Fig. 8. As shown, the LDA FS sheets of both isoelectronic systems exist in two Kramers double degenerated bands, (69,70) and (71,72), labeled by the numbers of the first band in each pair, i.e., 69 and 71, and are nearly identical for both systems, differing slightly only in the size of particular parts. They possess holelike and electronlike characters in the lower (69th) and higher (71st) of these bands, respectively. Which is worth underlining, the holelike sheets have a quasi-two-dimensional (Q2D) shape of squared cylinders with their axes along the line XR$\|c$ axis with nesting[15] vectors along the [100] direction—see Fig. 8. Thus, a weaker interaction between U atoms, solely contributing to the FSs, is expected along the elongated c axis. In turn, two kinds of electron sheets occur in the higher (71st) band of both studied ternaries. The first one has again a Q2D character with a shape of a corrugated cylinder but with its axis orientation along the AM$\|c$ line (at the edge of BZ) and the second one, forming a pillow, is centered at the Z point.

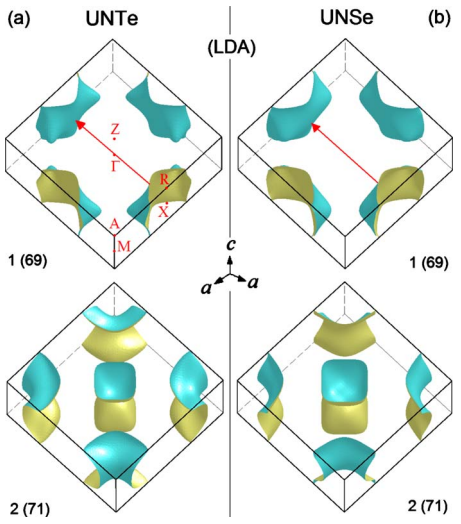

FIG. 8. (Color online) Calculated FS in the NMO (LDA) state of: (a) UNTe and (b) UNSe. For each compound FS sheets existing in two Kramers double-degenerated bands are numbered in brackets) and drawn separately in tetragonal BZ boundaries (with high-symmetry points and nesting vectors in red color). Dark (blue) and light (yellow) colors visualize the inside (electrons) and outside (holes) of FS, respectively.

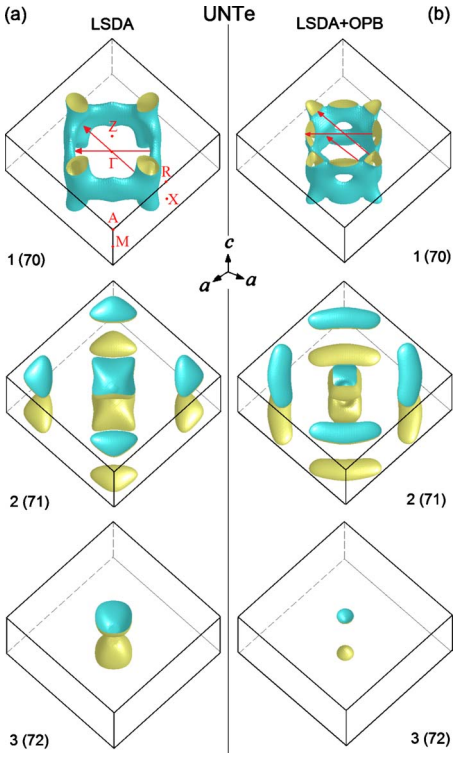

FIG. 9. (Color online) Calculated FS of ferromagnetic UNTe employing: (a) LSDA and (b) LSDA+OPB approaches. FS sheets exist in three nondegenerated bands, drawn in the same convention as in Fig. 8.

The Fermi surfaces of UNTe in the FM states (along the c axis), computed using both the LSDA and LSDA+OPB approaches, are visualized in Fig. 9. As is visible, the FS sheets obtained based on both approaches exist in three nondegenerated bands (70, 71, 72). In the 70th band, there are single holelike Q2D sheets originating from some topological transformation of the squared cylinders from the 69th double-degenerated LDA band due to removing the instability associated with the band points 1 and 2 (along the ΓM and RA lines, respectively) marked in Fig. 3 and discussed in the text. These new Q2D sheets possess also tetragonal symmetry and distinct nesting features[15] along the ΓM ([100]) and ΓX ([110]) directions marked by nesting vectors in the figure. Thus, this quasi-two-dimensionality of FS with nesting allows for arising additional exotic phenomena under special conditions (e.g., under pressure or doping). In the succeeding (71st) band, electronlike tetragonal pillows, centered at the Z point, are similar to those in the case of the LDA results presented in Fig. 8(a). Moreover, in this band there are electronlike pockets (LSDA) or cigars (LSDA+OPB), centered near the A point. They originate from a reduction in the cylindrical sheets existing in the same (71st) band as shown for the LDA results [see Fig. 8(a)]. Finally, in the upper (72nd) band, there are small electronlike spheres around the Z point.

The total ordered FM moments in UNTe (per one U atom), μ_{tot}, calculated along the easy magnetization c axis in

TABLE III. Spin (μ_s), orbital (μ_l), and total (μ_{tot}) FM moments for UNTe, aligned along the *c* axis, obtained using two different functionals.

	FM moments per one uranium atom (in μ_B)			
Functionals	μ_s	μ_l	μ_{tot}	Experimental $\lvert\mu_{tot}\rvert$
LSDA	0.70	−1.22	−0.51	0.85 ± 0.16 [a] or 1.2[b]
LSDA+OPB	0.87	−2.10	−1.23	

[a]Reference 4.
[b]Reference 3.

the LSDA and LSDA+OPB approximations, are given in Table III. The LSDA functional gives an underestimated value $|\mu_{tot}|=0.51\mu_B$ while the LSDA+OPB functional, yielding slightly overestimated $|\mu_{tot}|=1.23\mu_B$, improves agreement with an average experimental value of about $1.0\mu_B$.[3,4] It should be emphasized here that the LSDA+OPB approach is completely *ab initio* since it does not require any external fitting parameters, as e.g., *U* and *J* in the commonly used LSDA+*U non-ab initio* approaches. As demonstrated here, it is useful to reproduce electronic structure corresponding to medium values, just about $1.0\mu_B/1$ atom U, of ordered magnetic moments. When expecting higher values, another functional, LSDA+OPXC, containing the OP energy connected with orbital correlations,[16] is recommended, as shown previously for the U_2N_2(Sb,Te,Bi) ternaries.[8]

Summarizing, the band structure, DOS and FS figures for both compounds, UNTe and UNSe, look roughly the same in the LDA approach and merely slight differences can lead to an appearance of magnetic ordering in UNTe. For the latter system the OPB correction improves agreement with the experimental magnetic moments.

IV. CONCLUSIONS

Electronic and magnetic structures of the UN*Z*-type (*Z*=Te,Se) isostructural and isoelectronic ternary compounds have been computed employing the FPLO code. An atomic bonding of a covalently metallic character in both compounds was predicted by the calculations. Only the U 5*f* and 6*d* electrons create a metallic bond between uranium atoms lying in (001) layers but they contribute also to covalentlike bonding with the other ligand atoms. The band structures of both ternaries contain pseudogaps near E_F in the NMO states, which are reduced in UNTe in the FM spin- and orbital-polarized (LSDA+OPB) state, which stabilizes its metallic state. Also a collinear FM arrangement of uranium moments of $1.23\mu_B$ along the *c* axis is confirmed by computations as the ground state of UNTe, which exhibits half-metallic properties. Moreover, the calculations reveal that the U 5*f* electrons in this compound exhibit a *dual* character. The OPB version of the *ab initio* orbital polarization correction yields a good agreement with experiments for UNTe of the total magnetic moment on U atoms. Finally, the Fermi surfaces of these ternaries exhibit Q2D features with distinct nesting vectors along the [100] and [110] directions, which should influence their transport and magnetic properties. Based on the results, one expects in the future interesting physical measurements, performed on suitable samples, for these uniquely combining uranium and nitrogen (or oxygen) systems, containing also a chalcogen.

ACKNOWLEDGMENTS

I am grateful to R. Troć for critical reading of this paper and also thankful for a technical assistance by U. Nitzsche with IFW-Dresden computers, and by G. Banach and J. Wrzodak at the Computing Center of Institute of Low Temperature and Structure Research PAS in Wrocław.

[1] R. Trojko and Z. Despotović, Croat. Chem. Acta **47**, 121 (1975).
[2] R. Troć and Z. Żołnierek, J. Phys. (Paris) **40**, C4-79 (1979).
[3] R. Troć, Inorg. Chim. Acta **140**, 67 (1987).
[4] G. Amoretti, A. Blaise, P. Burlet, J. E. Gordon, and R. Troć, J. Less Common Met. **121**, 233 (1986).
[5] D. Kaczorowski, *Pnictides and Chalcogenides III (Ternary Actinide Pnictides and Chalcogenides)*, Landolt-Börnstein, New Series, Group III Vol. 27B8, edited by H. P. J. Wijn (Springer-Verlag, Berlin, 2004).
[6] R. Troć, *Pnictides and Chalcogenides III (Actinide Monopnictides)*, Landolt-Börnstein, New Series, Group III Vol. 27B6α, edited by H. P. J. Wijn (Springer-Verlag, Berlin, 2006), p. 74.
[7] M. Samsel-Czekała, E. Talik, P. de V. Du Plessis, R. Troć, H. Misiorek, and C. Sułkowski, Phys. Rev. B **76**, 144426 (2007).
[8] M. Samsel-Czekała, Phys. Rev. B **80**, 045121 (2009).
[9] P. Hohenberg and W. Kohn, Phys. Rev. **136**, B864 (1964); W. Kohn and L. J. Sham, *ibid.* **140**, A1133 (1965).
[10] FPLO5.00–18 and 5.10–20, http://www.FPLO.de; K. Koepernik and H. Eschrig, Phys. Rev. B **59**, 1743 (1999).
[11] OPB correction implementation in FPLO5.10–20 according to: O. Eriksson, M. S. S. Brooks, and B. Johansson, Phys. Rev. B **41**, 7311 (1990); Carsten Neise, Diploma thesis, Technische Universitat, Dresden, 2007.
[12] J. P. Perdew and Y. Wang, Phys. Rev. B **45**, 13244 (1992).
[13] J. Flahaut, J. Solid State Chem. **9**, 124 (1974).
[14] N. K. Sato, N. Aso, K. Miyake, R. Shiina, P. Thalmeier, G. Varelogiannis, C. Geibel, F. Steglich, P. Fulde, and T. Komatsubara, Nature (London) **410**, 340 (2001); G. Zwicknagl and P. Fulde, J. Phys.: Condens. Matter **15**, S1911 (2003).
[15] S. B. Dugdale, H. M. Fretwell, M. A. Alam, G. Kontrym-Sznajd, R. N. West, and S. Badrzadeh, Phys. Rev. Lett. **79**, 941 (1997); D. Hughes, M. Däne, A. Ernst, W. Hergert, M. Lüders, J. Poulter, J. B. Staunton, A. Svane, Z. Szotek, and W. M. Temmerman, Nature (London) **446**, 650 (2007).
[16] H. Eschrig, M. Sargolzaei, K. Koepernik, and M. Richter, Europhys. Lett. **72**, 611 (2005).